EES Solar

COMMUNICATION

View Article Online
View Journal

Cite this: DOI: 10.1039/d5el00206k

Received 11th December 2025
Accepted 5th January 2026

DOI: 10.1039/d5el00206k

rsc.li/EESSolar

Nickel-oxide hole-transport layers prevent abrupt reverse-bias breakdown and permanent shorting of perovskite solar cells caused by pinhole defects

Daniel A. Morales, Jr,[ab] Collin Sindt,[bc] Kell Fremouw,[ab] Kaitian Mao,[ab] Matteo Poma,[ab] Thomas Stewart,[d] Ryan A. DeCrescent [b] and Michael D. McGehee*[abc]

When perovskite solar cells (PSCs) are subjected to reverse bias, they often abruptly pass large current densities through localized film defects. The large, localized current induces heating that quickly and permanently damages the materials in the device – including transport layers, perovskite, and metal contacts – and often leads to permanent electrical shorting of the device. We employed a 30-nm-thick nickel oxide (NiO_X) hole transport layer (HTL) in PSCs and found that NiO_X decreased the likelihood that cells show abrupt reverse-bias breakdown and prevented permanent shorting and severe thermal damage. We found that cells using NiO_X could recover up to 84% of their initial PCE even after passing -20 mA cm^{-2} of average reverse current densities (the cell's one-sun short-circuit current density) for 5 minutes. Cells with all-organic HTLs were permanently shorted afterwards. In addition to preventing abrupt breakdown, photoluminescence images of cells before and after reverse-bias breakdown show that NiO_X also prevents localized damage to the perovskite and transport layers, presumably due to its superior uniformity and thermal stability compared to organic HTLs.

Broader context

When a solar panel is partially shaded, current can be forced "backward" through the shaded cells. This condition, known as "reverse bias", causes severe thermal and electrical stress even in strong silicon cells. Perovskite solar cells have historically been very weak to this type of stress, showing rapid and permanent degradation under slight reverse bias. In perovskite solar cells – like other thin-film solar cells – some of this problem is related to the use of very thin (5 to 10 nanometers) hole-transporting layers which have thickness inhomogeneities and pinholes that act as electrical weak spots. To improve their electrical and thermal resilience, they need to be thicker while avoiding excessive electrical resistance. We show that sputtered nickel oxide is a good material choice to make thicker hole transport layers that can solve this problem. Sputtered nickel oxide has exceptional uniformity and lower electrical resistance compared to solution-processed organic hole transport layers. It reliably makes perovskite solar cells more resilient to moderate reverse bias. Sputtering is also a relevant industry-scale process that can be used to deposit high-quality films over large areas, and even on highly textured silicon for perovskite-silicon tandem solar cells.

Perovskite solar cells (PSCs) have emerged as a leading contender in next-generation photovoltaics, demonstrating single-junction power conversion efficiencies (PCEs) above 26.9%, nearly matching the PCEs of the best crystalline silicon (Si) cells, and enabling PCEs beyond 34.8% in Si-perovskite tandem cells.[1] The commercialization of PSCs is largely limited by their instabilities under external stressors such as moisture, illumination, and temperature cycling.[2–7] Another important stressor that is receiving increasing attention is reverse bias, a condition which may occur in a series-connected cell during a partial shading event. PSCs in particular have demonstrated two distinct types of reverse bias breakdown: "gradual" breakdown in which current begins to exponentially and smoothly pass in reverse bias due to the tunneling of holes into the perovskite (usually around -4 to -5 V), and "abrupt" breakdown in which large currents arise at an unpredictable voltage up to several volts below the cell's tunneling breakdown voltage.[8,10,18,26,28] Abrupt breakdown often leads to immediate and severe localized damage.[8–10] Gradual breakdown due to hole tunneling is not as physically destructive as abrupt breakdown, but is associated with electrochemical degradation of the contacts, transport layers, and perovskite.

Abrupt breakdown of thin-film solar cells in reverse bias is typically associated with the formation of "hotspots" which occur near fabrication defects (*e.g.*, pinholes in any layer, or other electrically conductive defects), leading to low breakdown voltages of just -1 V to -4 V.[11–17] Pinholes and weak spots are a common result of crystallization dynamics (*e.g.*, bubbles or film tension), material defects (particle or dried material

[a]Materials Science and Engineering (MSE) Program, University of Colorado Boulder, Boulder, CO 80303, USA. E-mail: Michael.McGehee@colorado.edu; dmo7603@gmail.com

[b]Renewable and Sustainable Energy Institute (RASEI), University of Colorado Boulder, Boulder, CO 80303, USA. E-mail: Ryan.Decrescent@colorado.edu

[c]Chemical and Biological Engineering, University of Colorado Boulder, Boulder, CO 80303, USA

[d]Department of Physics, University of Colorado Boulder, Boulder, CO 80309, USA

attachment) or poor wetting of the solution on the substrate.[19–21] Commercial Si cells have high reverse breakdown voltages (V_{Br}) – often greater than −15 V – and panels can thus be protected against reverse-bias stress by incorporating about one bypass diode per 10–20 cells. The low and unpredictable V_{Br} in typical PSCs (sometimes as low as −0.5 V to −1 V) would not reliably enable the bypass diode strategy, and would in the best case still require about one bypass diode per cell, greatly increasing production costs.[19] Any strategy to reliably increase breakdown voltages to several volts will be helpful in this regard. Strategies to increase the V_{Br} of PSCs have involved using a tin-oxide (SnO_X) electron transport layer (ETL) or using a thicker (∼35 nm) polymer hole-transport layer (HTL) to improve layer uniformity and eliminate conductive weak spots. With these strategies, V_{Br} values have been increased up to about −10 to −12 V or larger.[18,22] However, thick undoped polymers increase series resistance and reduce power-conversion efficiencies to unacceptable levels, while doped polymers can introduce parasitic optical absorption.[23]

Here, we show that sputtered NiO_X is a good HTL for preventing abrupt breakdown in PSCs. A 30-nm-thick layer of NiO_X provides uniform coverage on rough transparent conductive oxides (TCOs) like tin-doped indium oxide (ITO), and has low optical loss and acceptably low series resistance. The thermal stability of NiO_X compared to organic HTLs also allows it to pass larger localized current densities and experience larger localized Joule heating without catastrophic failure, helping prevent permanent shorting even if cells show abrupt breakdown. Because of its improved uniformity over organic HTLs, it is also reasonable to assume that if pinholes are present within the perovskite layer, the current would be more evenly distributed across the entire pinhole, or even the whole cell, rather than highly localized at an HTL "weak" spot in the perovskite pinhole. We used photoluminescence (PL) imaging before and after reverse biasing cells to locate pinhole defects in the perovskite film that are likely passing disproportionately large localized current densities under reverse bias. PL imaging shows that NiO_X prevents damage to the perovskite around these pinholes.

Results & discussion

In perovskite pinholes, direct contact between the HTL and ETL allows this region to be an alternate pathway for current flow between the electrodes of the solar cell. These regions have diode-like current–voltage behavior (Fig. 1A). We refer to these junctions as "transport layer diodes" (TLDs). Measuring the current–voltage behavior of these perovskite-free TLDs provides useful information about the quality and uniformity of the transport layers and their ability to resist large current densities in perovskite pinholes. We first qualify NiO_X as a good choice for reverse-bias stability by fabricating and measuring the reverse-bias behavior of perovskite-free TLDs composed of ITO, an HTL, a C_{60} fullerene/bathocuproine (BCP) ETL, and Ag top contact (SI). The HTLs comprised either NiO_X, a "self-assembled monolayer" (SAM), or a combination of the two ('NiO_X + SAM'). NiO_X can be combined with a SAM, here [4-(3,6-dimethyl-9*H*-carbazol-9-yl)butyl]phosphonic acid (Me-4PACz), to reduce the surface recombination velocity, prevent reactions between the perovskite and NiO_X, and enable cells to reach higher efficiencies.[24,25] We compared that behavior to TLDs fabricated without NiO_X (*i.e.*, with only SAMs). The reverse current density–voltage (*J–V*) curves are shown in Fig. 1B. These measurements involved gradually sweeping the voltage from 0 V to negative voltages until the devices passed an average current density equal to −20 mA cm^{-2}, approximately the short-circuit current density (J_{SC}) of our solar cells.

NiO_X significantly reduced the chance of abrupt reverse breakdown in TLDs compared to SAM-only HTLs. 11 out of 12 TLDs using NiO_X (including NiO_X and NiO_X + SAM) showed a gradual reverse-bias breakdown (blue and grey curves). Further, the NiO_X TLDs retained their diode-like *J–V* behavior after these reverse bias scans, indicating no permanent degradation to the materials in the TLD during reverse bias (Fig. 1C). In contrast, all SAM-only TLDs showed abrupt breakdown before reaching −2 V (Fig. 1B) and were permanently shorted afterward (Fig. 1C). In a complete solar cell, we expect NiO_X or NiO_X + SAM HTLs to help prevent abrupt breakdown and permanent device degradation should perovskite pinholes exist.

Having established that TLDs comprising NiO_X show consistent reverse-bias *J–V* behavior and gradual reverse-bias breakdown, we compared solar cells with a combination of NiO_X and NiO_X + SAM HTLs to ones with a SAM-only HTL. Initial forward-bias *J–V* sweeps show that PCEs of NiO_X + SAM devices (17.46 ± 1.08%) were similar to those with SAMs (18.81 ± 1.01%) (Fig. 1D). Devices with SAMs showed on average slightly higher open-circuit voltages due to improved interface properties (1180.7 ± 35.6 mV for SAM devices and 1175.5 ± 30.9 mV for NiO_X + SAM devices). 30 nm of NiO_X did not add appreciable series resistance to the cells. During the reverse-bias *J–V* sweeps, the PSCs with NiO_X + SAM HTLs were much more likely to show gradual breakdown around −4 V to −5 V (Fig. 1E).[26,28] Breakdown statistics are presented in Fig. 1F, where we bin the total number of cells based on the voltage at which they pass −20 mA cm^{-2} average current density. NiO_X + SAM PSCs show a substantially higher proportion of devices exceeding −4 V (9 out of 11 devices) compared to SAM-only devices (3 out of 11 devices). NiO_X + SAM PSCs also showed more consistent and gradual breakdown behavior.

To assess cells for any permanent damage after these reverse-bias *J–V* scans, we tested the forward-bias performance of the cells under illumination. PSCs comprising a SAM-only HTL showed an average PCE loss of 65.1% (relative) after reverse-bias *J–V* scans. In contrast, cells with NiO_X + SAM HTL showed an average PCE loss of 47.8% (relative) afterward and displayed fewer instances of highly conductive ohmic shunts (SI Fig. 1). The PCE losses were primarily driven by reduced shunt resistances and associated reduced fill factors (FFs).

To understand the degradation of the cells after reverse bias, we delaminated the Ag electrodes from the cells and performed X-ray photoelectron spectroscopy (XPS) on both the peeled electrodes and the underlying perovskite films (SI Fig. 2 and 3). The XPS spectra from the peeled Ag electrodes (SI Fig. 2) showed I 3d signals after reverse bias, regardless of the HTL used. Since

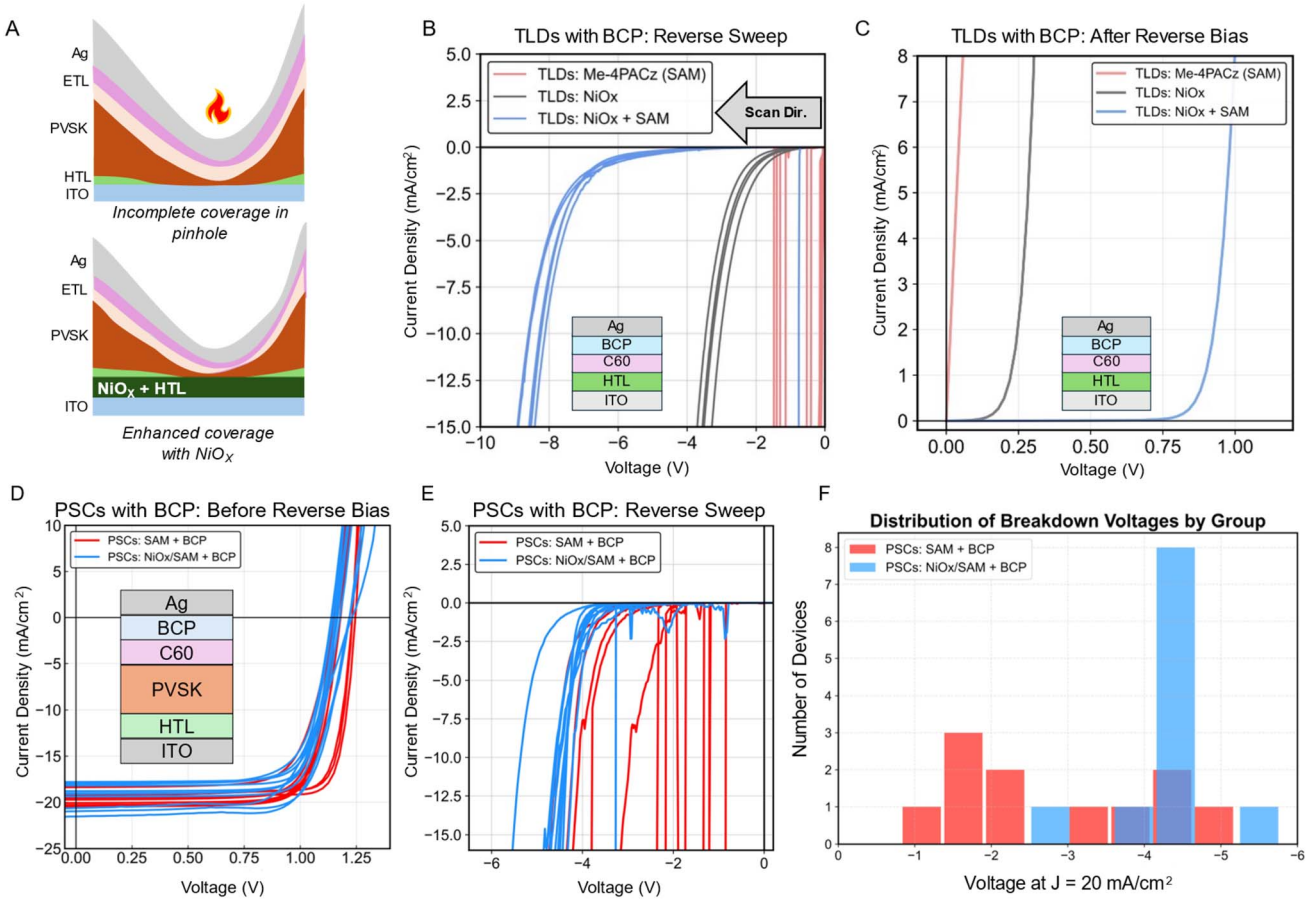

Fig. 1 (A) Illustration of a pinhole within a PSC with (bottom) and without (top) NiO_X in the HTL. (B) Reverse current density–voltage (J–V) scans of TLDs with HTLs comprising NiO_X (black), Me-4PACz (red) ("SAM"), and NiO_X + SAM (blue). (inset) The perovskite-free TLD architecture tested. (C) Forward J–V scans measured after reverse J–V scans shown in panel B. (D) Light-J–V scans of complete PSCs with NiO_X + SAM (blue) and SAM-only (red) HTLs before reverse bias. (inset) The device architecture tested. (E) Reverse J–V scans of the PSCs shown in panel D. (F) Reverse breakdown statistics of each device architecture extracted from panel E (the total number of devices based on the voltage at which they pass -20 mA cm^{-2} average current density).

neutral iodine would likely leave the sample as a gas, the signal is likely from the formation of AgI at the Ag/BCP/C_{60} interface due to the diffusion of iodine (I^-, I_2, or I_3^-) through the C_{60} occurring during reverse bias. A thin layer of AgI would be electrically resistive and would likely change energy alignment between the metal and ETL, decreasing the J_{SC} and FF. This would be especially true in cells that did not show abrupt breakdown during reverse J–V sweeps since they experienced larger reverse potentials over longer periods of time. Visual images of the perovskite films below the delaminated Ag electrodes after reverse bias show some type of surface corrosion and optical scattering texture (SI Fig. 2B), further support the hypothesis of AgI formation.

The observations from both Fig. 1 and from XPS (SI Fig. 2 and 3) show that although NiO_X helps prevent abrupt low-voltage breakdown in PCSs, it does not prevent harmful electrochemistry at the ETL and top metal contact interface associated with the soft breakdown of the cells. To prevent the formation of AgI and associated degradation in our PSCs, we used atomic layer deposition (ALD) to deposit a 20-nm-thick SnO_X ETL on top of the C_{60} layer. ALD SnO_X is well known to be an excellent ETL material and barrier against diffusion of metal and iodine in PSCs.[18,22,27] We used the same HTL combinations, perovskite layer, and Ag top metal contact (Fig. 2A).[15,20]

When using ALD SnO_X with any HTL combination, the average reverse breakdown voltages shift to larger reverse potentials by about -1 V, but the portion of abrupt breakdown events still depends on the specific HTL (Fig. 2B). We found that abrupt breakdown still frequently occurs for the SAM-only HTL PSCs during the reverse J–V scans (Fig. 2B, red curves). In contrast, NiO_X once again consistently reduced the likelihood of abrupt breakdown (blue and black curves). The breakdown statistics are shown in Fig. 2C, where we again bin the total number of devices based on the voltage at which they pass -20 mA cm^{-2} average current density. SAM-only HTLs led to 8 out of 19 (42%) exceeding -4.5 V, whereas NiO_X and NiO_X + SAM HTLs led to 7 out of 9 (78%) and 15 out of 16 (93%) devices exceeding this voltage before breaking down, respectively. The J–V curves before and after the reverse sweeps for each HTL with ALD SnO_X are provided in SI Fig. 4.

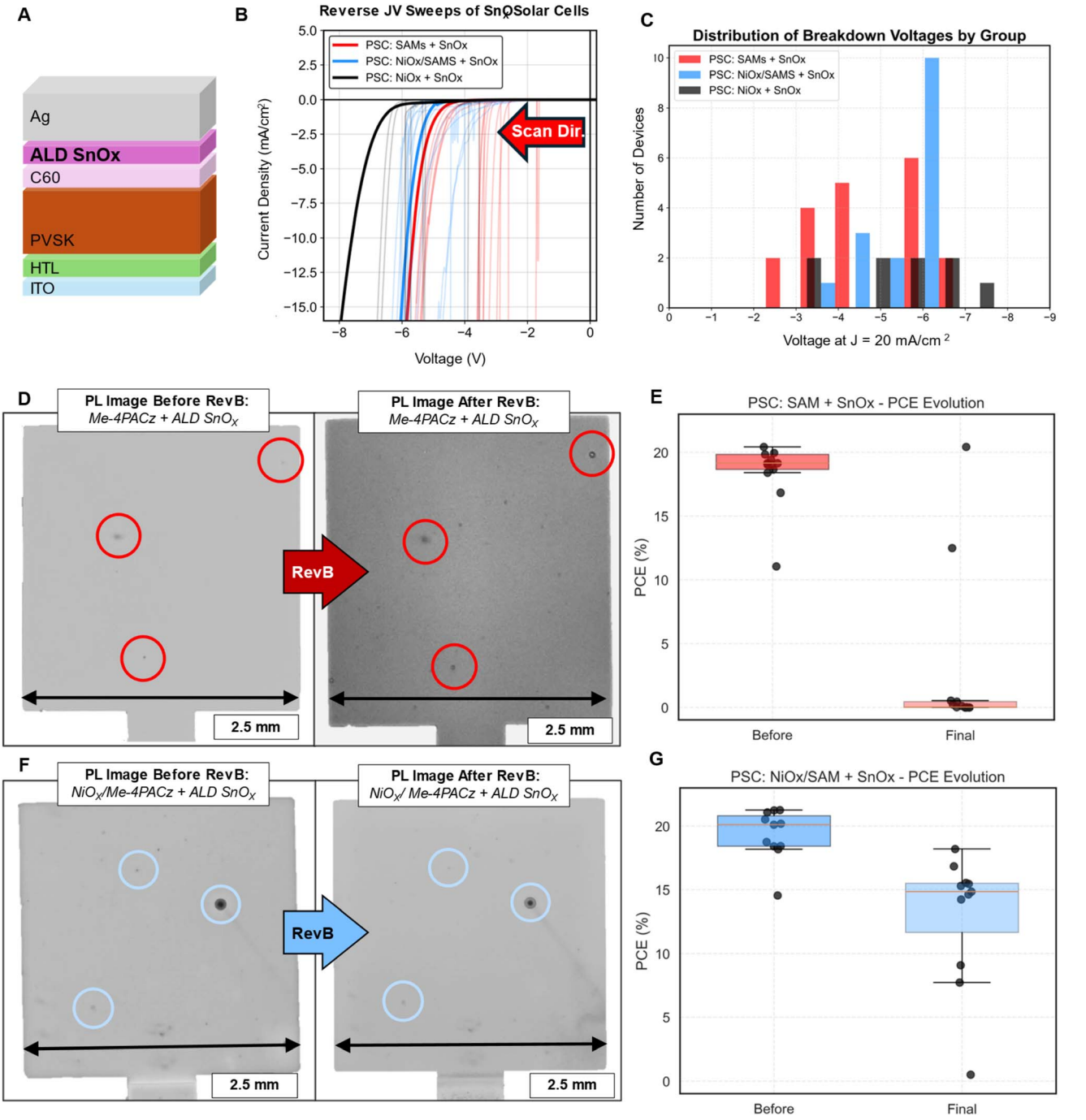

Fig. 2 (A) Schematic of the solar cell device stack including ALD SnO_X. (B) Reverse-bias J–V curves of solar cells with three different HTL combinations. The single curve with the highest breakdown voltage for each architecture is presented with a bold line style. The rest are fainter, thin curves. (C) Reverse breakdown statistics of solar cells comprising three different HTL combinations extracted from panel B (SAM HTLs (red bins), $n = 19$; NiO_X + SAMs (blue bins), $n = 16$; bare NiO_X (black bins), $n = 9$). (D) PL images of a solar cell with SAM-only HTL before (left) and after (right) reverse bias. Circles highlight identified pre-existing pinhole defects. (E) PCE statistics of solar cells before and after holding an average current density of -20 mA cm^{-2} (-2.4 mA) through the cell for 5 minutes in the dark. (F and G) Equivalent to panels D & E, instead with a NiO_X + SAM HTL combination.

NiO_X once again prevented the abrupt breakdown of our solar cells during these reverse bias scans. Nearly all cells with SnO_X ETLs were not permanently shunted after these reverse J–V sweeps. We attribute the improved ability of the cells to retain their PCEs to the ALD SnO_X layer, which acts as a strong barrier against ion diffusion, helping to prevent the formation of AgI under reverse bias, and preventing the formation of permanent conductive shunts even if cells showed abrupt breakdown for short durations.[18,27]

To better understand the resilience of NiO_X, we stressed a separate batch of cells by passing −2.4 mA through the cell – corresponding to an average current density of −20 mA cm^{-2} (their approximate J_{SC}) – in the dark for both 5 and 20 minutes. If the current is distributed disproportionately with high localized current densities in pinholes, we expect very high temperatures and cell degradation in those regions. After holding these cells at −2.4 mA for 5 minutes in the dark, we performed light-*J*–*V* scans in forward bias and found that 10 out of 11 cells with NiO_X retained some degree of photovoltaic performance, on average retaining 75% of their initial PCEs (Fig. 2E) (exemplary *J*–*V* curves before and after a long fixed-current stress test is shown in SI Fig. 6). In contrast, nearly all cells (9 out of 11) with SAM-only HTLs remained permanently shorted (Fig. 2G). We further investigated the cause of the degradation of cells with organic HTLs by PL imaging to look for evidence of burn marks or permanent damage. In contrast to visual microscopy, PL images can indicate subtle localized degradation to the perovskite layer that is revealed by decreased PL intensity. A net decrease in PL intensity across the cell can also reveal highly conductive shunts between the electrodes.

We were particularly interested in damage occurring at pre-existing pinholes, which was previously identified to be the origin of substantial material degradation and even electrode melting.[18] Fig. 2D shows PL images of a PSC with a SAM-only HTL before (left) and after (right) holding −2.4 mA for 20 minutes in the dark. Several pre-existing perovskite pinholes are circled, identified by dark spots in the PL image. After reverse-bias stress, we observed a slight exaggeration of these same defects, indicating that degradation of the perovskite occurred in these areas. On average, PL intensities across the whole cell area decreased after reverse bias, indicating highly conductive permanent shunts. Voltage–time curves for these fixed-current holds are shown in SI Fig. 5, where abrupt decreases in the applied potential indicate some type of abrupt breakdown during the measurements. Forward-bias *J*–*V* curves of these cells with SAMs showed linear behavior with a high slope and nearly 0% PCE even after allowing the devices to rest overnight (SI Fig. 7), indicating highly conductive permanent shorting from the formation of severe hotspots, burning and metal melting around these pinholes. In contrast, cells including NiO_X + SAM HTLs could be held at an average current density of −20 mA cm^{-2} for 20 minutes with no indication of burning, melting or other damage (Fig. 2F). Further, they showed no noticeable decrease in PL intensity across the whole cell area.

Without a uniform NiO_X layer, Joule heating likely leads to quick material degradation of the organic HTL, exposing the underlying ITO and leading to a run-away increase in current densities, metal melting and ultimately a permanently shorted cell like those shown in Fig. 2. Incorporating NiO_X underneath the SAM prevents the formation of highly conductive contact between ITO and the ETL and seems to prevent extreme localized heating, burning and melting.

Conclusions

It will be challenging to make full-size solution-processed perovskite solar panels that do not have perovskite pinholes. From our measured statistics on 0.12 cm^2 cells (Fig. 1E) and from EL images (Fig. 2D and F), we estimate approximately 20–25 cm^{-2} for the density of pinholes that lead to abrupt breakdown in cells without NiO_X (SI). With a 30 nm NiO_X HTL, the density of these catastrophic defects effectively decreases to <1 cm^{-2}. A thick NiO_X HTL can thus be thought of as a way to "passivate" defects that lead to abrupt breakdown. It is therefore important to implement robust electron and hole transport layers that reliably separate the two electrodes so that abrupt breakdown does not result in severe and permanent thermal damage when cells are exposed to negative bias. We investigated the impact of using a 30-nm-thick layer of sputtered NiO_X for this purpose and found that NiO_X reduced the likelihood of abrupt breakdown caused by perovskite pinholes and HTL defects in the cell. To test the thermal stability and current-handling capability of NiO_X compared to all-organic HTLs, we forced cells to pass their short-circuit current densities in the dark for 5 minutes and found that NiO_X prevented permanent damage to the perovskite and prevented the formation of permanent, highly conductive shunts in the cells. NiO_X is a good choice for a robust HTL because a 30-nm-thick layer has acceptably low parasitic absorption, acceptably low series resistance, and can reliably cover roughness in a TCO electrode. Although we did not make devices on textured silicon for the purpose of making perovskite-Si tandems for this study, sputtered NiO_X should be more effective for this application than typical solution processing methods. It is well known that perovskite-NiO_X interfaces have relatively high surface recombination velocity and undesirable chemical reactions. It is therefore desirable to combine NiO_X with a material that passivates the NiO_X-perovskite interface, such as a SAM, so that high power conversion efficiency and robustness against abrupt reverse bias breakdown can both be obtained. Our study showed that the combination NiO_X/Me-4PACz HTL also prevents permanent device shorting after abrupt breakdown. The combination of NiO_X HTLs with SnO_X ETLs offers superior reverse bias stability even if perovskite pinholes exist.

Conflicts of interest

McGehee is an advisor to Swift Solar.

Data availability

Data for this article, including forward and reverse current–voltage curves, are available Mendeley Data. DOI: https://doi.org/10.17632/8wybb48284.1.

Supplementary information (SI): experimental details (materials, device fabrication, and characterization), additional data, and modeling. See DOI: https://doi.org/10.1039/d5el00206k.

Acknowledgements

This research was funded by the National Science Foundation (NSF) under award number DMR 2245435. XPS measurements were performed at COSINC-CHR, CU Boulder

(RRID:SCR_018985). We thank the Keck Lab at JILA for support and resources related to NiO_X fabrication.

References

1 Interactive Best Research-Cell Efficiency Chart | Photovoltaic Research | NREL, https://www.nrel.gov/pv/interactive-cell-efficiency.

2 L. Duan, D. Walter, N. Chang, J. Bullock, D. Kang, S. P. Phang, K. Weber, T. White, D. Macdonald, K. Catchpole, *et al.*, Stability challenges for the commercialization of perovskite–silicon tandem solar cells, *Nat. Rev. Mater.*, 2023, **8**(4), 261–281, DOI: 10.1038/s41578-022-00521-1.

3 S. G. Ji, I. J. Park, H. Chang, J. H. Park, G. P. Hong, B. K. Choi, J. H. Jang, Y. J. Choi, H. W. Lim, Y. J. Ahn, *et al.*). Stable pure-iodide wide-band-gap perovskites for efficient Si tandem cells via kinetically controlled phase evolution, *Joule*, 2022, **6**, 2390–2405, DOI: 10.1016/J.JOULE.2022.08.006.

4 R. Li, L. Yao, J. Sun, Z. Sun, K. Zhang, J. Xue and R. Wang, Challenges and perspectives for the perovskite module research, *Chem*, 2025, 102542, DOI: 10.1016/J.CHEMPR.2025.102542.

5 D. J. Slotcavage, H. I. Karunadasa and M. D. McGehee, Light-Induced Phase Segregation in Halide-Perovskite Absorbers, *ACS Energy Lett.*, 2016, **1**, 1199–1205, DOI: 10.1021/ACSENERGYLETT.6B00495/ASSET/IMAGES/LARGE/NZ-2016-004953_0007.JPEG.

6 E. T. Hoke, D. J. Slotcavage, E. R. Dohner, A. R. Bowring, H. I. Karunadasa and M. D. McGehee, Reversible photo-induced trap formation in mixed-halide hybrid perovskites for photovoltaics, *Chem. Sci.*, 2014, **6**, 613–617, DOI: 10.1039/C4SC03141E.

7 T. Seyisi, B. G. Fouda-Mbanga, J. I. Mnyango, Y. B. Nthwane, B. Nyoni, S. Mhlanga, S. P. Hlangothi and Z. Tywabi-Ngeva, Major challenges for commercialization of perovskite solar cells: A critical review, *Energy Rep.*, 2025, **13**, 1400–1415, DOI: 10.1016/J.EGYR.2025.01.019.

8 A. R. Bowring, L. Bertoluzzi, B. C. O'Regan and M. D. McGehee, Reverse Bias Behavior of Halide Perovskite Solar Cells, *Adv. Energy Mater.*, 2018, **8**, 1702365, DOI: 10.1002/AENM.201702365.

9 L. Bertoluzzi, C. C. Boyd, N. Rolston, J. Xu, R. Prasanna, B. C. O'Regan and M. D. McGehee, Mobile Ion Concentration Measurement and Open-Access Band Diagram Simulation Platform for Halide Perovskite Solar Cells, *Joule*, 2020, **4**, 109–127, DOI: 10.1016/j.joule.2019.10.003.

10 L. Bertoluzzi, J. B. Patel, K. A. Bush, C. C. Boyd, R. A. Kerner, B. C. O'Regan, M. D. McGehee, L. Bertoluzzi, K. A. Bush, C. C. Boyd, *et al.*). Incorporating Electrochemical Halide Oxidation into Drift-Diffusion Models to Explain Performance Losses in Perovskite Solar Cells under Prolonged Reverse Bias, *Adv. Energy Mater.*, 2021, **11**, 2002614, DOI: 10.1002/AENM.202002614.

11 S. J. Heise, A. Komilov, M. Richter, B. Pieters, A. Gerber and J. Neerken, Reverse-bias behaviour of thin-film solar cells: effects of measurement-induced heating, *EPJ Photovoltaics*, 2023, **14**, 17, DOI: 10.1051/EPJPV/2023008.

12 M. Nardone, S. Dahal and J. M. Waddle, Shading-induced failure in thin-film photovoltaic modules: Electrothermal simulation with nonuniformities, *Sol. Energy*, 2016, **139**, 381–388, DOI: 10.1016/J.SOLENER.2016.10.006.

13 J. Bauer, J. M. Wagner, A. Lotnyk, H. Blumtritt, B. Lim, J. Schmidt and O. Breitenstein, Hot spots in multicrystalline silicon solar cells: Avalanche breakdown due to etch pits, *Phys. Status Solidi RRL*, 2009, **3**, 40–42, DOI: 10.1002/PSSR.200802250.

14 M. Igalson, P. Zabierowski, D. Przado, A. Urbaniak, M. Edoff and W. N. Shafarman, Understanding defect-related issues limiting efficiency of CIGS solar cells, *Sol. Energy Mater. Sol. Cells*, 2009, **93**, 1290–1295, DOI: 10.1016/J.SOLMAT.2009.01.022.

15 P. Szaniawski, P. Zabierowski, J. Olsson, U. Zimmermann and M. Edoff, Advancing the Understanding of Reverse Breakdown in Cu(In,Ga)Se2 Solar Cells, *IEEE J. Photovolt.*, 2017, **7**, 1136–1142, DOI: 10.1109/JPHOTOV.2017.2699860.

16 T. J. Silverman, M. G. Deceglie, X. Sun, R. L. Garris, M. A. Alam, C. Deline and S. Kurtz, Thermal and Electrical Effects of Partial Shade in Monolithic Thin-Film Photovoltaic Modules, *IEEE J. Photovolt.*, 2015, **5**, 1742–1747, DOI: 10.1109/JPHOTOV.2015.2478071.

17 E. Palmiotti, S. Johnston, A. Gerber, H. Guthrey, A. Rockett, L. Mansfield, T. J. Silverman and M. Al-Jassim, Identification and analysis of partial shading breakdown sites in CuInxGa(1-x)Se2 modules, *Sol. Energy*, 2018, **161**, 1–5, DOI: 10.1016/J.SOLENER.2017.12.019.

18 S. Johnson, D. Morales, K. Fremouw, I. E. Gould, T. Borsa, S. Johnston, A. Palmstrom, R. A. DeCrescent and M. D. McGehee, How non-ohmic contact-layer diodes in perovskite pinholes affect abrupt low-voltage reverse-bias breakdown and destruction of solar cells, *Joule*, 2025, 102102, DOI: 10.1016/J.JOULE.2025.102102.

19 D. E. Bornside, C. W. Macosko and L. E. Scriven, Spin coating: One-dimensional model, *J. Appl. Phys.*, 1989, **66**, 5185–5193, DOI: 10.1063/1.343754.

20 Z. Zhu, J. Lowes, J. Berron, B. Smith and D. Sullivan, Spin-Coating Defect Theory and Experiments, *ECS Trans.*, 2014, **60**, 293–302, DOI: 10.1149/06001.0293ECST/XML.

21 S. G. Kim, J. H. Kim, P. Ramming, Y. Zhong, K. Schötz, S. J. Kwon, S. Huettner, F. Panzer and N. G. Park, How antisolvent miscibility affects perovskite film wrinkling and photovoltaic properties, *Nat. Commun.*, 2021, **12**(1), 1–10, DOI: 10.1038/s41467-021-21803-2.

22 N. Li, Z. Shi, C. Fei, H. Jiao, M. Li, H. Gu, S. P. Harvey, Y. Dong, M. C. Beard and J. Huang, Barrier reinforcement for enhanced perovskite solar cell stability under reverse bias, *Nat. Energy*, 2024, **9**(10), 1264–1274, DOI: 10.1038/s41560-024-01579-7.

23 V. M. Le Corre, M. Stolterfoht, L. Perdigón Toro, M. Feuerstein, C. Wolff, L. Gil-Escrig, H. J. Bolink, D. Neher and L. J. A. Koster, Charge Transport Layers Limiting the Efficiency of Perovskite Solar Cells: How to Optimize Conductivity, Doping, and Thickness, *ACS Appl.*

Energy Mater., 2019, **2**, 6280–6287, DOI: 10.1021/ACSAEM.9B00856/ASSET/IMAGES/LARGE/AE9B00856_0004.JPEG.

24 Y. Guo, L. Huang, C. Wang, J. Huang, S. Liu, X. Liu, J. Zhang, Z. Hu and Y. Zhu, Efficient inverted perovskite solar cells with a low-temperature processed NiOx/SAM hole transport layer, *J. Mater. Chem. C*, 2024, **12**, 1507–1515, DOI: 10.1039/D3TC03575A.

25 Q. Cao, T. Wang, X. Pu, X. He, M. Xiao, H. Chen, L. Zhuang, Q. Wei, H. L. Loi, P. Guo, *et al.*). Co-Self-Assembled Monolayers Modified NiOx for Stable Inverted Perovskite Solar Cells, *Adv. Mater.*, 2024, **36**, 2311970, DOI: 10.1002/ADMA.202311970.

26 Z. Xu, H. Bristow, M. Babics, B. Vishal, E. Aydin, R. Azmi, E. Ugur, B. K. Yildirim, J. Liu, R. A. Kerner, *et al.*). Reverse-bias resilience of monolithic perovskite/silicon tandem solar cells, *Joule*, 2023, **7**, 1992–2002, DOI: 10.1016/j.joule.2023.07.017.

27 S. A. Johnson, K. P. White, J. Tong, S. You, A. Magomedov, B. W. Larson, D. Morales, R. Bramante, E. Dunphy, R. Tirawat, *et al.*). Improving the barrier properties of tin oxide in metal halide perovskite solar cells using ozone to enhance nucleation, *Joule*, 2023, **7**, 2873–2893, DOI: 10.1016/J.JOULE.2023.10.009.

28 F. Jiang, Y. Shi, T. R. Rana, D. Morales, I. E. Gould, D. P. McCarthy, J. A. Smith, M. G. Christoforo, M. Y. Yaman, F. Mandani, *et al.*, Improved reverse bias stability in p–i–n perovskite solar cells with optimized hole transport materials and less reactive electrodes, *Nat. Energy*, 2024, **9**(10), 1275–1284, DOI: 10.1038/s41560-024-01600-z.